RSC Advances

ROYAL SOCIETY OF CHEMISTRY

www.rsc.org/advances

Graphical abstract

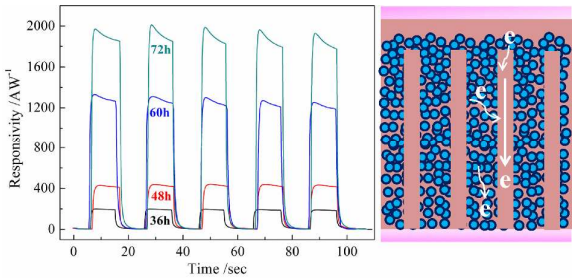

The large surface area from TiO_2 nanoparticles, well-defined electron transport pathway from TiO_2 nanorods and the homojunction formed at the interface contribute the hierarchical composite a fast and high photoresponse.

A High Responsive UV Photodetector Based on Hierarchical TiO_2 Nanorod /Nanoparticle Composite

Wenji Zheng [a], Xiangcun Li [a], Gaohong He [a]*, Xiaoming Yan [a], Rui Zhao [a], Chunxu Dong [b]

[a] *State Key Laboratory of Fine Chemicals, The R&D Center of Membrane Science and Technology, Dalian University of Technology, Dalian, 116012，China.*

[b] *College of Chemistry and Chemical Engineering, Lanzhou University, Lanzhou, 730000, China.*

*Corresponding author

E-mail address: hgaohong@dlut.edu.cn, Tel: +86-0411-84986291, Fax: +86-0411-84986291

Abstract

Hierarchical TiO_2 nanorod/nanoparticle composites were successfully prepared by $TiCl_4$ modification of vertically aligned TiO_2 nanorod (NR) arrays. After the hydrolysis of $TiCl_4$ at room temperature, TiO_2 nanoparticles (NPs) were deposited on the surface of TiO_2 NRs. Morphology and structure analysis demonstrated that the TiO_2 NPs were distributed around the whole surface of TiO_2 NRs, due to the easy permeation of $TiCl_4$ solution between the NRs space. Besides, the high concentration of $TiCl_4$ and long reaction time are favorable for the generation of more TiO_2 NPs, which correspondingly increase the surface area of the composite to a large extent. Compared with most reported TiO_2 based UV photodetectors (PDs), the present TiO_2 NR/NP composite based PDs exhibit an extremely high responsivity and a relatively fast response speed simultaneously. The maxima of responsivity and response speed are obtained from the sample of TiO_2 NR/NP-0.4M-72h, which are 1973 AW^{-1} and 0.47s (rise time) as well as 1.02s (decay time), respectively. The fast and high photoresponse are ascribed to the large surface area provided by TiO_2 NPs, the well-defined electron transport pathway offered from TiO_2 NRs and the homojunction formed at the interface between them. Moreover, together with the high responsivity and the relatively fast response speed, the significant UV light selectivity and a very good linear relationship between photoresponse and UV light intensity suggest the present UV PDs is very competitive and highly applicable in UV light detection.

1 Introduction

Ultraviolet (UV) light photodetectors (PDs) have drawn increasing attention in the past decade due to their various industrial and scientific applications, including communications, remote control, environmental monitoring, binary switches in imaging techniques, chemical/biological sensing, as well as in future memory storage and optoelectronic circuits.[1-5] As the most common and commercial UV PDs, Si-based photodiodes exhibit some intrinsic limitations, such as low responsivity and difficulty of blocking out visible and infrared photons, owing to their small band gap energies.[6] To enhance the UV responsivity and selectivity (visible blindness), people paid special attention on wide band gap semiconductors, such as GaN, SiC, ZnO and TiO_2.[7]

Titanium dioxide (TiO_2), a wide band gap n-type semiconductor (anatase 3.2 eV and rutile 3.0 eV), has been widely studied in the areas of photocatalysis, light emission diodes, solar cells and gas sensors, due to its excellent chemical, optical and electronic properties [8-11]. The distinctive ultraviolet (UV) absorption characteristics make TiO_2 an attractive candidate for UV detection against the background of infrared and/or visible light. According to the photoconductive mechanism, TiO_2 based UV PDs are typically divided into two categories, which are photoconductors and photodiodes (Schottky barrier, p-n junction and metal-semiconductor-metal structure). Compared with photodiodes based PDs, photoconductors exhibit large photoconductive gain and high photoresponsivity. However, slow response speed limits their applications very much. In most of the studies, it is hard to obtain high responsivity and fast response speed at the same time. For example, Xue et al. [6] demonstrated a nanocrystalline TiO_2 film PD with Au Schottky contacts, showing a high responsivity of 199 AW^{-1} at 260 nm. Kong [7] prepared a MSM TiO_2 PD and found a high responsivity of 899.6 AW^{-1} to UV light. However, the response times in their studies are tens of seconds which is too long to be applied. Xing et al. [12] fabricated epitaxial TiO_2 thin

films on $LaAlO_3$ as MSM PD and obtained the fast rise time of 8 ns but a relatively low responsivity of 3.63 AW^{-1} at 310nm. Li et al. [13] showed a TiO_2/SnO_2 heterojunction based self-powered UV PDs with a rise time of 0.03s and decay time of 0.01s, but with a low responsivity of 0.6 AW^{-1}. So it is important to get UV PDs with both high responsivity and fast response speed.

Recently, one-dimensional (1D) TiO_2 nanostructures have been extensively studied as UV PDs, because of the well-defined carrier transport pathway. [14] For example, He et al. [15] obtained a responsivity of 5.8×10^{-3} AW^{-1} based on vertically aligned TiO_2 nanorods (NRs) on Ti foil as UV PDs. Tsai et al. [16] presented a TiO_2 nanowire based PD and obtained a low resposivity of ~10^{-5} AW^{-1}. The low responsivity was due to the low surface area of TiO_2 NRs or nanowires, which not only reduced the UV photon absorption efficiency of TiO_2, but also lowered the depth of charge depletion produced by the oxygen adsorption at the surface of TiO_2. Zou et al. [17] took use of anodic TiO_2 nanotube arrays as UV PDs, and achieved a higher responsivity of 13 A/W at 2.5V bias with rise and decay time of 0.5 and 0.7s, respectively. The high responsivity was ascribed to oxygen adsorption and desorption induced by the large surface area of TiO_2 nanotubes. Therefore, it is obvious that the surface area is an important factor to enhance photoresponse of TiO_2 based UV PDs. Although TiO_2 based UV PDs were improved a lot, the responsivity and response speed are still not high enough for commercial application, and further improvement in the responsivity and response speed is quite necessary. As is well known, TiO_2 nanoparticles (NPs) have exhibited higher photoelectric conversion efficiency than 1D TiO_2 nanostructures in solar cells, because of their large surface area. Therefore, it is most desirable to maintain both the direct pathway for fast electron transfer provided by TiO_2 1D nanostructures and the large surface area for sufficient oxygen adsorption and photon absorption offered from TiO_2 NPs.

Herein, TiO_2 NR/NP hierarchical composite film was prepared for UV light detection. Well

aligned TiO_2 NR arrays were first synthesized on FTO glass by hydrothermal method, and TiO_2 NPs were then filled into the TiO_2 NR array interspace by hydrolysis of $TiCl_4$ at room temperature. Compared with either TiO_2 NRs or TiO_2 NPs based UV PDs, the hierarchical composite film based PDs showed a significant improvement in the photoresponsivity, photosensitivity and response speed.

2 Experimental

2.1 Hydrothermal growth of TiO_2 NRs arrays

As described in ref. [18], in a typical synthesis, 26 mL of deionized water was mixed with 26 mL of hydrochloric acid (37% by weight) under stirring for 5 min. Then a certain amount of titanium isopropylate (TIP) was added dropwise and stirred for another 5 min. The precursor was transferred into a Teflon-lined autoclave (80 mL), and then two pieces of FTO (14 Ω cm^{-2}) glass were immersed into the solution at an angle against the wall with conductive side facing down. The hydrothermal reaction was carried out at 180¤for 4h in an electric oven. After synthesis, the autoclave was cooled to room temperature by flowing water, and then the FTO glasses were taken out and rinsed with deionized water thoroughly, followed by ambient air drying.

2.2 Deposition of TiO_2 NPs among TiO_2 NRs by hydrolysis of $TiCl_4$

The TiO_2 NPs were deposited between TiO_2 NRs through solution growth method by immersing the TiO_2 NRs samples in an aqueous solution of $TiCl_4$ for different reaction times. [19] The samples were immersed in 0.1M, 0.2 M and 0.3M $TiCl_4$ solution at room temperature for 24, 36, 48, and 60h, respectively. After immersion, the samples were rinsed with absolute ethanol and deionized water several times, and then were annealed in air at 450℃ for 30 min in a furnace.

2.3 UV PD assembly

The UV PD was assembled by sandwiching hierarchical TiO_2 NR/NP composite film between two FTO conductive glasses. The active area of the PD is 0.98cm^2. The measurements of the current-voltage (I-V) characteristics and the photoresponse of the devices were conducted with an IviumStat Electrochemical Station under irradiation of a portable mercury lamp (Spectroline, ENF-280C/FA) with 365 nm wavelength. The UV light intensity was obtained by optical power meter (Newport, 1916-R).

2.4 Characterization

Morphologies of TiO_2 NRs and TiO_2 NPs are characterized by a field-emission scanning electron microscope (FE-SEM, NOVA NanoSEM 450, FEI). Crystal structures were examined by X-ray diffraction (XRD) using an X-ray diffraction meter (Philips X'pert, Holland) with Cu Ka radiation (λ =1.5418 A). Transmission electron microscopy (TEM) and high-resolution TEM (HR-TEM) analyses were performed on a high resolution transmission electron microscope (Tecnai G2 F30 S-Twin, FEI).

3. Results and discussion

3.1 Morphology and structure of TiO_2 NRs, NPs and their hierarchical composite

The XRD patterns of the pristine TiO_2 NRs and NPs as well as three representative TiO_2 NR/NP composites are shown in Fig. 1. It is obvious that all the diffraction peaks of the five samples are well indexed to the standard tetragonal rutile structure of TiO_2 (PDF file #01-086-0147), no diffraction peaks of impurities are observed. Compared with TiO_2 NPs, the significantly high intensity of (002) peak of TiO_2 NRs demonstrates that the as-prepared TiO_2 NR arrays are highly oriented on FTO substrates. After the modification of TiO_2 NPs, the relative intensity of the (002) peaks of the TiO_2 NR/NP composite becomes weaker, which could be attributed to the large number of TiO_2 NPs around the oriented nanorods. Furthermore, the relative intensity of the (002) peaks of the TiO_2 NR/NP composite decreases

with the treatment time of $TiCl_4$ solution increasing, indicating more and more TiO_2 NPs produced.

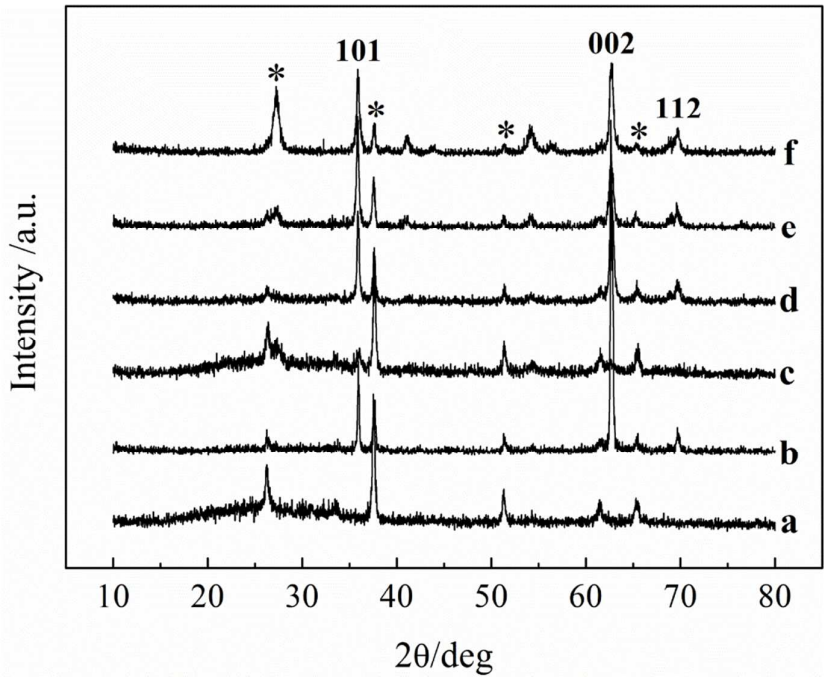

Fig.1 XRD pattern of TiO_2 samples: (a) FTO glass, (b)TiO_2 NRs, (c) TiO_2 NPs, (d) TiO_2 NR/NP-0.2M-36h, (e) TiO_2 NR/NP-0.2M-48h, (f) TiO_2 NR/NP-0.2M-60h, TiO_2 NRs is prepared at 180¤, 0.7ml TIP for 4h and TiO_2 NPs is obtained at $TiCl_4$ concentration of 0.2M for 60h

The TEM images of some individual TiO_2 NRs modified by TiO_2 NPs in Fig.2 further demonstrate that a large amount of TiO_2 NPs are generated around the TiO_2 NRs by the hydrolysis of $TiCl_4$. Fig. 2(a) shows a large number of rod-like TiO_2 NPs distribute around a TiO_2 NR and the diameter and length of TiO_2 NP are about 10 nm and 50 nm, respectively. The high resolution TEM image of some TiO_2 NPs in Fig. 2(b) indicates that TiO_2 NPs are rutile TiO_2, which is consistent with the result of XRD.

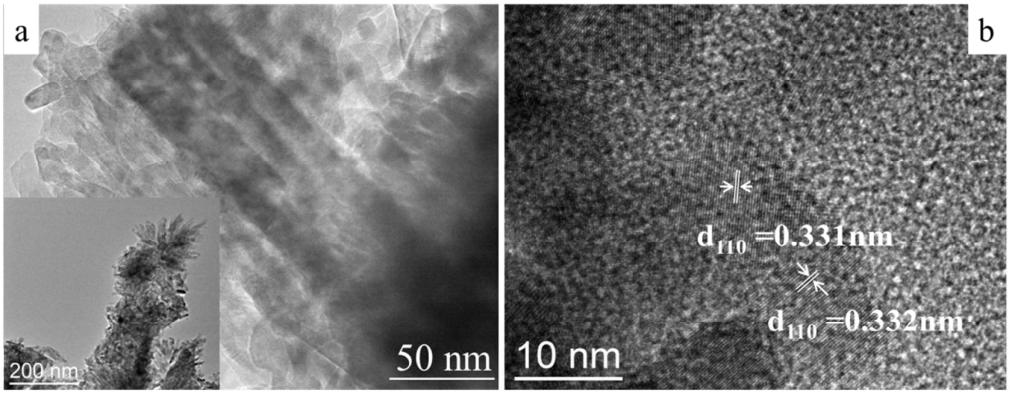

Fig.2 TEM and HR-TEM images of TiO_2 NR/NP composite

FE-SEM images of TiO_2 NRs modified by TiO_2 NPs at different treatment time and different $TiCl_4$ concentration (marked as TiO_2 NR/NP-xM-xh) are represented in Fig. 3. From the top views of TiO_2 NR/NP-0.2M-(24-60) h in Fig.3 (a-d), it is clearly seen that the top surfaces of the NRs are covered with a large number of TiO_2 NPs and the surfaces become rough. Additionally, the diameters of the TiO_2 NRs covered with TiO_2 NPs increase obviously with the treatment time increasing, which is caused by the increasing amount of the TiO_2 NPs deposited on the TiO_2 NRs. When the treatment time reaches 60h, many large TiO_2 NP aggregates (~0.5μm) deposit on the top surface of TiO_2 NRs, which is too thick to stick together very well. This phenomenon would have a negative impact on the photoresponse of TiO_2 based UV PDs. With the treatment time increasing, the cross-sectional views in Fig. 3(e-h) show that the TiO_2 NPs can also penetrate through the space between the NRs and distribute around the NRs, due to the easy permeation of $TiCl_4$ aqueous solution. When the treatment time reaches 60h, the TiO_2 NR layer is hardly seen in the cross-sectional image due to the quite thick TiO_2 NPs layer on it. When the $TiCl_4$ concentration is 0.3 M, the dependence of morphology of TiO_2 NR/NP on the modification time is the same as that of 0.2 M $TiCl_4$, as shown in Fig. 3(i-k). When the treatment time is extended to 60h, much more TiO_2 NPs distribute around TiO_2 NRs and this would greatly increase the surface area of the

TiO_2 NR/NP composite. While at the treatment time of 72h, some cracks appear on the top of TiO_2 NRs, indicating that an excess of TiO_2 NPs generated. At the $TiCl_4$ concentration of 0.4 M, the composite exhibits a more compact top view than that of TiO_2 NR/NP-0.3M-60h, demonstrating a further increase of TiO_2 NPs. The above results reveal that the longer growth time and the higher concentration of $TiCl_4$ solution could give rise to a larger amount of TiO_2 NPs on the NRs, which would increase the specific surface area of TiO_2 NR/NP composite, therefore improving the photoresponse of TiO_2 NR/NP based UV PDs.

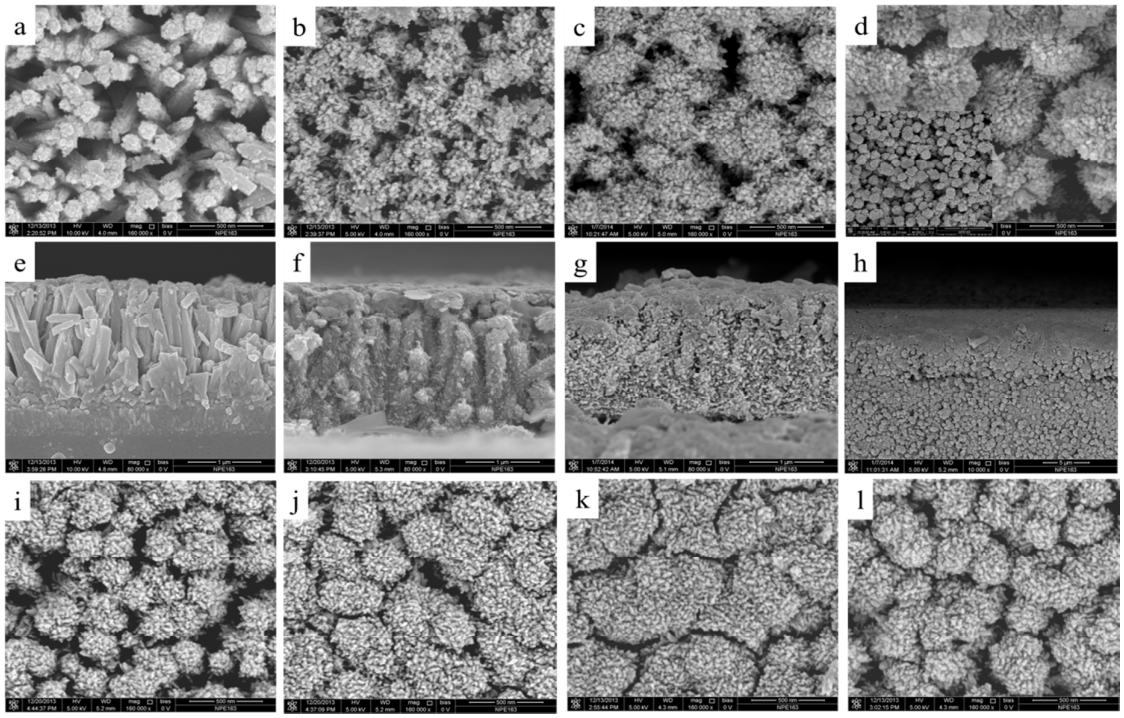

Fig.3 FE-SEM images of TiO_2 NR/NP-0.2M-24h (a, e), TiO_2 NR/NP-0.2M-36h (b, f), TiO_2 NR/NP-0.2M-48h (c, g), TiO_2 NR/NP-0.2M-60h (d, h), TiO_2 NR/NP-0.3M-48h (i), TiO_2 NR/NP-0.3M-60h (j), TiO_2 NR/NP-0.3M-72h (k), and TiO_2 NR/NP-0.4M-72h (l). The inset is the low-resolution view of the sample (d)

UV-Visible absorption spectra are presented in Fig. 4 to verify the visible light blindness of TiO_2 NR/NP composite based UV PDs. The absorption edges of TiO_2 NRs, NPs and the composites are all around 410 nm, which is consistent with that of the bulk rutile TiO_2 (412

nm). The maximum absorption peaks of TiO_2 NRs and NPs are 368 nm and 349 nm, respectively. Compared with TiO_2 NRs, the absorption peak of TiO_2 NPs shows a blue shift due to the quantum size effect.[20] And those of the composite lie between the above two values, gradually approaching 349 nm of TiO_2 NPs with the growth time increasing, which again suggests that more TiO_2 NPs are produced with the growth time prolonged.

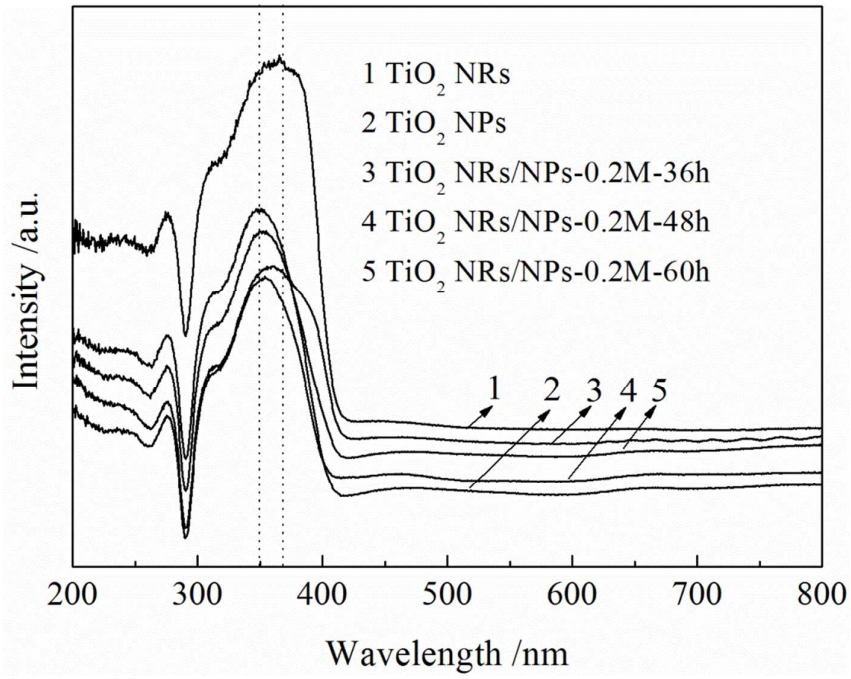

Fig.4 UV-Vis absorption spectra of TiO_2 NRs, TiO_2 NPs and their hierarchical composite at $TiCl_4$ concentration of 0.2M

Fig. 5(a) shows the I-V response curve of TiO_2 NRs modified by TiO_2 NPs at $TiCl_4$ concentration of 0.2 M and at growth time from 0h to 60h in the dark and under the illumination of 365nm UV light. It is clearly seen that the dark currents of TiO_2 NR/NP based UV PDs are all in the magnitude of 10^{-7}A, while the photocurrents of TiO_2 NR/NP based UV PDs are significantly higher than that of only TiO_2 NRs based PDs. Furthermore, the photocurrents of TiO_2 NR/NP based UV PDs increase with the growth time of TiO_2 NPs increasing. With the growth time approaching 48h, the photocurrent exhibits a maximum of

0.15 mA, which is 155 times higher than that of TiO_2 NRs based PDs. With the growth time further extended to 60 h, the photocurrent decreases and approaches to the value of TiO_2 NR/NP-24h. The first increase in the photocurrent is attributed to the large surface area provided by the increasing amount of TiO_2 NPs, which improves the photon absorption efficiency and surface related electron-hole separation efficiency. The next decrease in the photocurrent is resulted from the thick TiO_2 NPs layer on the surface of TiO_2 NRs, which produces losses incurred by charge hopping across nanograin boundaries in the TiO_2 NPs layer. The effect of growth time of TiO_2 NPs on the photoresponse is further illustrated in the time response characteristics curves, as shown in Fig. 5(b-d). From all the three figures, it can be seen that when the UV light is turned on, an obvious photoresponsivity (defined as the photocurrent generated per unit power of incident light on the effective area of a photodetector) is generated for each sample. The five time response characteristics for each sample suggest an excellent stability and repeatability of the as-designed UV PDs. In the cases of TiO_2 NRs modified by 0.2 M $TiCl_4$ solution as shown in Fig. 5(b), with the modification time of TiO_2 NPs increasing from 0h to 48h, the responsivity increases gradually, and reaches a maximum of 194 AW^{-1}, which is much higher than the commercial values (0.1-0.2AW^{-1}). [21] As the modification time is increased to 60 h, the responsivity decreases to 34 AW^{-1}, close to that of the TiO_2 NR/NP-24h composite. The decrease in the responsivity is probably resulted from the trap-mediated hopping process of the charge carriers in the NPs and the tunneling of the charge carriers between adjacent NPs. As for the sample of TiO_2 NR/NP-48h, the photosensitivity (defined as the ratio of photocurrent to dark current) reaches 135, which is 13 times higher than that of TiO_2 NRs based PDs. The high photosensitivity is attributed to the large surface area provided by TiO_2 NPs and the well-defined electron transport pathway offered from TiO_2 NRs. In the other two cases of TiO_2 NRs modified by 0.3 M and 0.4 M $TiCl_4$ solution, as shown in Fig. 5(c, d), the dependence of

responsivity of TiO_2 NR/NP composite on the growth time of TiO_2 NPs exhibits the same trend as that of TiO_2 NRs modified by 0.2 M $TiCl_4$ solution. With respect to the sample of TiO_2 NR/NP-0.3M-xh, the maximum responsivity of 822 AW^{-1} is obtained when the growth time is 60h. As the growth time reaches 72h, the responsivity decreases due to the cracks formed on the top of TiO_2 NRs, as seen in Fig. 3(k). What's more, for the sample of TiO_2 NR/NP-0.4M-72h, the responsivity and photosensitivity are increased to 1973 AW^{-1} and 1158, respectively, which is related to the increasing amount and much smaller size of TiO_2 NPs generated by hydrolysis of $TiCl_4$ at high concentration and enough time.

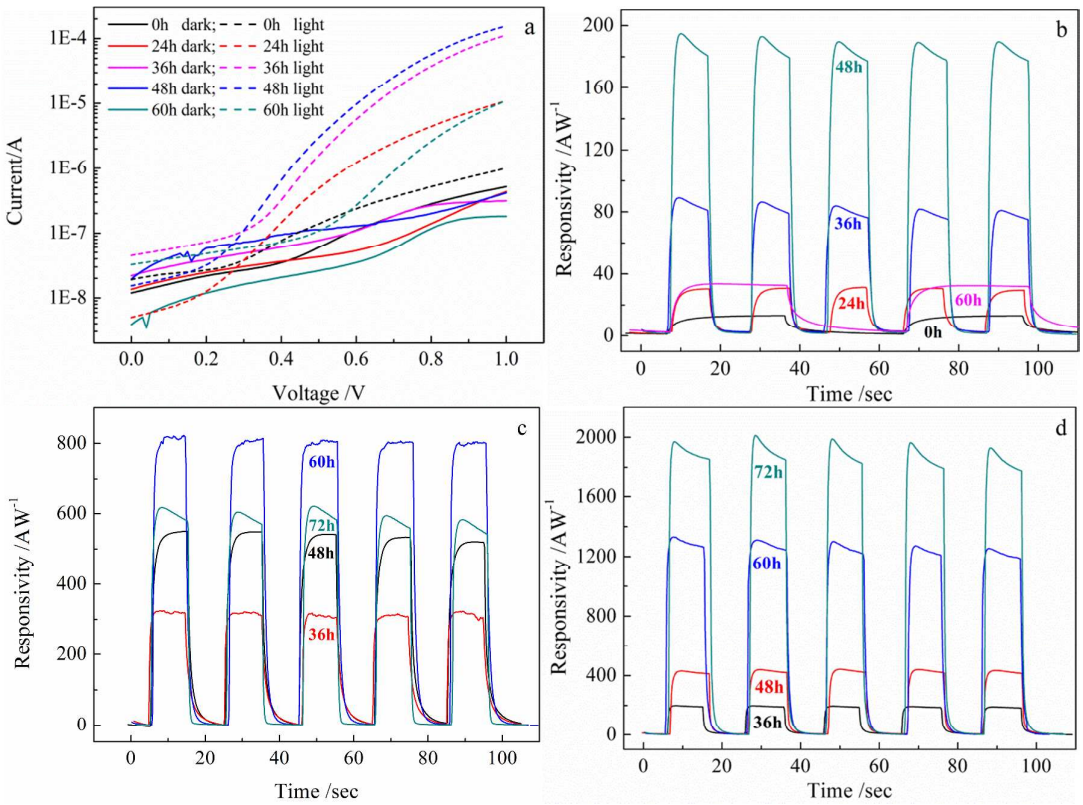

Fig.5 Responsive characteristics of TiO_2 NRs decorated by TiO_2 NPs at different $TiCl_4$ concentration and different reaction time under the illumination of 365nm UV light at 1.0V bias, (a) I-V curve at $TiCl_4$ concentration of 0.2M, (b) I-t curve at $TiCl_4$ concentration of 0.2M, (c) I-t curve at $TiCl_4$ concentration of 0.3M and (d) I-t curve at $TiCl_4$ concentration of 0.4M

Response speed is another important factor which is responsible for the high properties of

PDs. The response speeds of present hierarchical TiO_2 NR/NP composite based UV PDs are summarized in table 1. For the pristine TiO_2 NRs, the rise (defined as the time for the photocurrent increases from 10% to 90%) and decay time (defined as the time for the photocurrent decreases from 90% to 10%) is 8.7 s and 24.06 s respectively. At 0.2M $TiCl_4$ solution, with the growth time of TiO_2 NPs increasing from 24h to 48h, the rise and decay time decrease gradually, and reach a minimum of 1.46s and 1.40s at the growth time of 48h. As the growth time further extended, both of the rise and decay time increased, especially the decay time. The fastest response speed in this study is obtained from the sample of TiO_2 NR/NP-0.4M-72h, where the rise and decay time are 0.47s and 1.02s, respectively. In the meanwhile, the responsivity and photosensitivity achieve the maximum of 1973 AW^{-1} and 1159, respectively. Compared with most reported TiO_2 based UV detectors, as listed in table 2, the hierarchical TiO_2 NR/NP PDs exhibit the extremely high responsivity and relatively fast response speed at the same time, which is rarely found in the literature. The high performance could probably be ascribed to the straight electron transport path offered from one dimensional TiO_2 NRs, large surface area provided by TiO_2 NPs and the homojunction formed in the interface between TiO_2 NRs and NPs.

Tab.1 Responsive parameters of TiO_2 NRs modified by TiO_2 NPs at different $TiCl_4$ concentration and reaction time under the illumination of 365nm UV light at 1.0V bias

TiO_2 NRs/NPs	Rising time (s)	Decay time (s)	Responsivity (AW^{-1})	Photosensitivity
TiO_2 NRs-0h	8.63	25.02	13.18	10.77
0.2M-24h	2.64	4.77	30.81	23.51
0.2M-36h	1.13	1.48	89.13	35.68
0.2M-48h	1.07	1.18	194.82	135.24
0.2M-60h	3.7	20.85	34.52	12.37
0.3M-60h	0.96	1.57	821.78	684
0.4M-60h	0.6	1.19	1331.8	950.29
0.4M-72h	0.47	1.02	1973.09	1158.9
TiO_2 NPs-0.3M-60h	12.07	6.36	21.37	55.54

Tab.2 Comparison of TiO_2 nanostructure based UV PDs performance

TiO_2 nanostructure	Driving force(V)	Rising time (s)	Decay time (s)	Responsivity (AW^{-1})	Sensitivity	Ref.
NR/NP	1	0.47	1.02	1973	$>10^3$	This work
Nanorod	0	—	—	5.85×10^{-5}	—	[15]
Nanowire	5	—	—	6.85×10^{-5}	$\sim10^2$	[16]
Nanotube	2.5	0.5	0.7	13	$\sim10^4$	[17]
Nanofilm	5	0.55	0.38	~30	$\sim10^5$	[22]
Thin film	10	~8 ns	~90 ns	3.63	$\sim10^5$	[12]
Thin film	5	0.01	11.43	889.6	$\sim10^4$	[7]
Thin film	5	6	15	199	—	[6]
Heterojunction	0	0.03	0.01	0.6	$\sim10^3$	[13]

As is well accepted, the chemi-adsorption and photo-desorption of oxygen molecules on the surface of TiO_2 NRs are responsible for their photoresponse. In the dark, the oxygen molecules are adsorbed on the surface of TiO_2, capture the free electrons in the conductive band of TiO_2 and then a depletion layer with low conductivity is formed near the surface. [23] Under the illumination of UV light, electro-hole pairs are generated in TiO_2 NRs. Along the potential difference produced by band bending, the photogenerated holes migrate to the TiO_2 NR surface and then discharge the negatively charged oxygen ions by surface electron-hole recombination. Those unpaired electrons transport to the external circuit under the applied bias to produce current.

The high responsivity and relatively fast response speed in the composite are probably the results of the photoconductive gain and a homojunction formed at the interface. It is widely accepted that the contact between TiO_2 nanostructures and FTO glass is ohmic, so is the present TiO_2 NR/NP composite. [24-26] Thus the photoconductive gain is responsible for the present high responsivity [27]. The significant increase in responsivity after the modification of TiO_2 NPs could be attributed to two reasons. First, the increasing amount of light absorption provided by TiO_2 NPs induces an additional production of photogenerated electron hole pairs. Second, synergistic effect between TiO_2 NRs and NPs plays a crucial role

in enhancing the responsivity. In the TiO_2 NR/NP composite, as shown in Fig. 6(a), TiO_2 NR act as a conducting wire to quickly deliver the electron produced by TiO_2 NPs to the positive electrode, which not only prolongs the electron lifetime, but also enhances the electron transit speed. Both of them contribute to a high responsivity. Moreover, the I-V rectifying curve of TiO_2 NRs and NPs shown in Fig. 6(b) demonstrates that a homojunction could be formed in the contacting interface, probably due to the quantum confinement effect of the charge carriers in the TiO_2 NPs, resulting in the higher conduction and lower valence bands of the TiO_2 NPs than those of the TiO_2 NW. [20, 28] The possible homojunction provides an internal potential gradient to further accelerate the separation of the electron-hole pairs. This process is favorable for the relatively fast response speed. Nevertheless, it is needed to further study the mechanism of the homojunction in details.

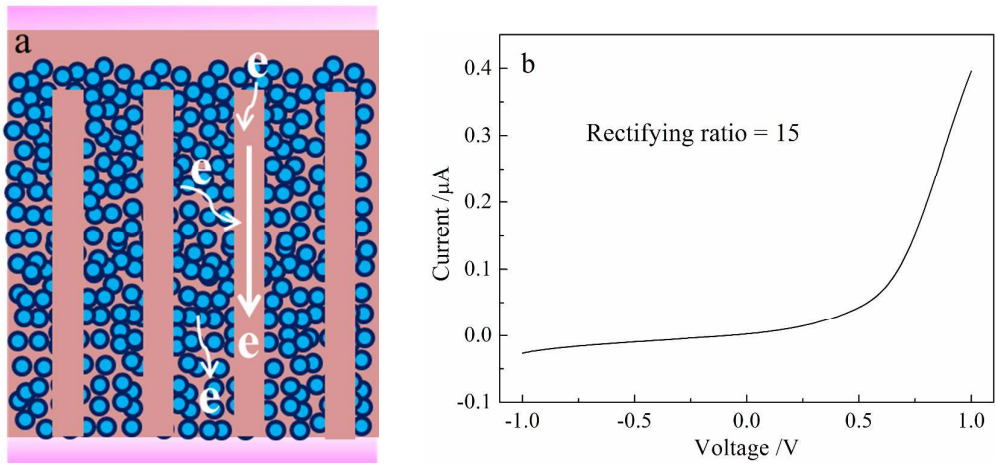

Fig.6 (a) Schematic of electron transport path in the TiO_2 NR/NP hierarchical composite, (b) I-V rectifying curve of TiO_2 NRs and TiO_2 NPs film on the FTO conductive glass

The dependence of photocurrent on incident light intensity shown in Fig. 7(a) gives another important characteristic of the TiO_2 based UV PDs. The photocurrent increases with the UV light intensity increasing from 135 to 556 nW/cm^2. Linear fitting result in Fig. 7(b) shows a fabulous linear dependence of photocurrent on the light intensity. It is worth noting

that the TiO_2 NR/NP-0.2M-48h based UV PDs exhibit a photocurrent of ~80μA and a photosensitivity of ~100 even in the ultralow light intensity of 135 nW/cm^2, indicating an excellent UV response behavior under low light intensity. Fig. 7(c, d) shows the spectral response of TiO_2 NR/NP-0.2M-48h at 1.0V bias. From the figure, it is clearly seen that this UV PD has peak response at 365nm and relatively low response at 254nm, but almost no response at the visible light region from 460 to 660nm, indicating an excellent UV light selectivity, which is in good agreement with the UV-Vis absorption of TiO_2.

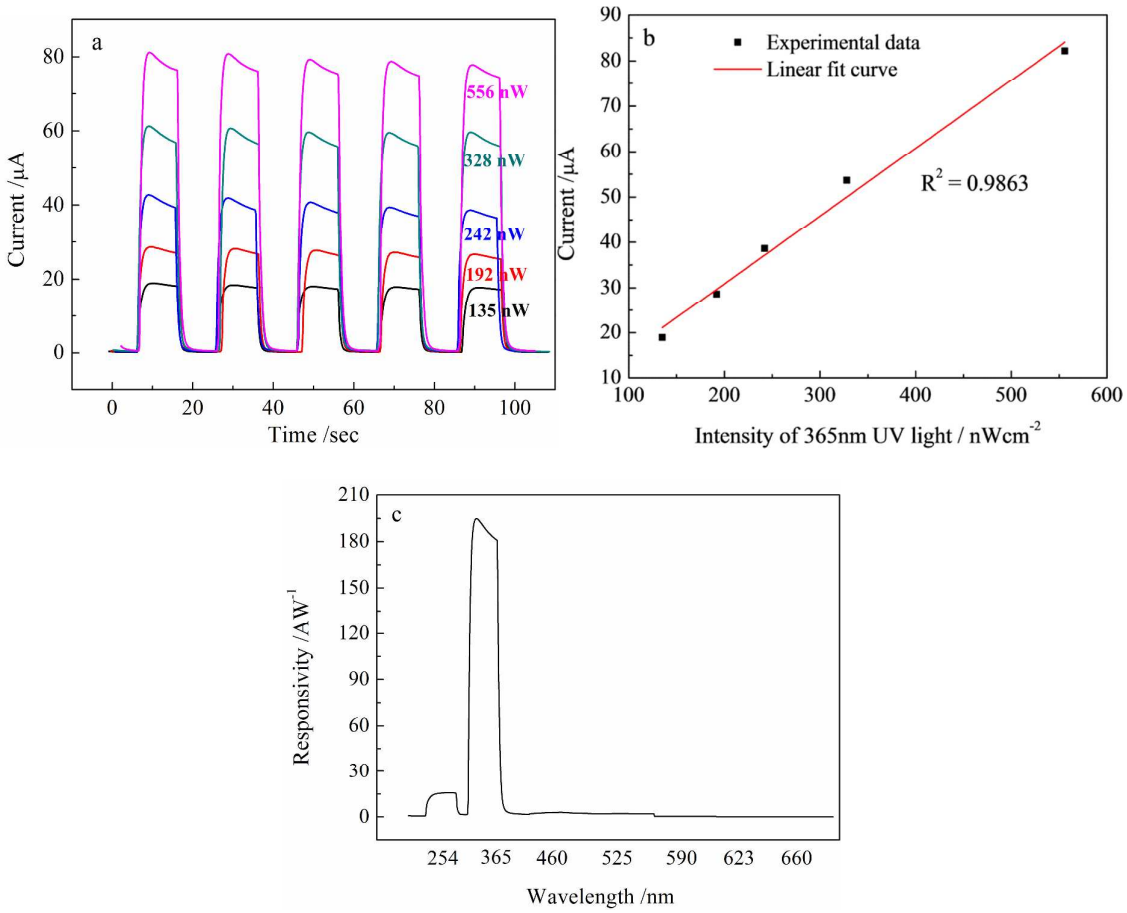

Fig.7 Effect of UV light intensity and light wavelength on the photoresponse of TiO_2 NR/NP-0.2M-48h sample at 1.0V bias, (a, b) UV light intensity responsive curve, (c) spectral responsive curve.

Conclusions

In summary, ordered TiO_2 NR arrays on the FTO conductive glass have been synthesized by simple hydrothermal method. TiO_2 NP modified TiO_2 NR hierarchical composites were obtained by hydrolysis of $TiCl_4$ at different concentrations for different reaction time. The TiO_2 NPs not only deposited on the top surface of TiO_2 NRs, but also filled the interface among the TiO_2 NRs, due to the easy permeation of $TiCl_4$ solution. High $TiCl_4$ concentration and long reaction time are favorable for the generation of more TiO_2 NPs, which enhance the surface area of the composite. Compared with most other studies, the TiO_2 NR/NP hierarchical composite based UV PDs exhibit an extremely high responsivity and relatively fast response speed at the same time. Among the samples, TiO_2 NR/NP-0.4M-72h based UV PD gives the highest responsivity of $1973AW^{-1}$, the largest photosensitivity of 1158.9 and the fastest response speed (The rise and decay time are 0.47s and 1.02s, respectively). The present high responsivity and relatively fast response speed are attributed to the large surface area generated by TiO_2 NPs, the straight electron transport pathway offered from TiO_2 NRs and the homojunction formed in the interface between TiO_2 NRs and NPs. Furthermore, the excellent dependence of photoresponse of the TiO_2 composite on the light intensity and the fabulous UV light selectivity all make it a good candidate for the UV light detection application.

Acknowledgements

The work was supported by the National Natural Science Fund for Distinguished Young Scholars of China (21125628) and the Fundamental Research Funds for the Central Universities (lzujbky-2013-61).

Reference

[1] S. Kim, Y. T. Lim, E. G. Soltesz, A. M. DeGrand, J. Lee, A. Nakayama, J. A. Parker, T. Mihaljevic, R. G. Laurence, D. M. Dor, L. H. Cohn, M. G. Bawendi and J. V. Frangioni, *Nat. Biotechnol.*, 2004, 22, 93.

[2] M. Ettenberg, *Adv. Imaging*, 2005, 20, 29.

[3] B. Tian, X. Zheng, T. J. Kempa, Y. Fang, N. Yu, G. Yu, Huang and C. M. Lieber, *Nature*, 2007, 449, 885.

[4] Y. Bie, Z. Liao, H. Zhang, G. Li, Y. Ye, Y. Zhou, J. Xu, Z. Qin, L. Dai, and D. Yu, *Adv. Mater.*, 2011, 23, 649.

[5] B. Tian and C. M. Lieber, *Pure Appl. Chem.*, 2011, 83, 2153.

[6] Z. Yu and M. Aceves-Mijares, *Appl. Phys. Lett.*, 2009, 95, 081101.

[7] X. Kong, C. Liu, W. Dong, X. Zhang, C. Tao, L. Shen, J. Zhou, Y. Fei, and S. Ruan, *Appl. Phys. Lett.*, 2009, 94, 123502.

[8] C. Lin, Y. Song, L. Cao and S. Chen, *Nanoscale*, 2013, 5, 4986.

[9] B. O'Regan and M. Gratzel, *Nature*, 1991, 353, 737.

[10] P. Docampo, S. Guldin, M. Stefik, P. Tiwana, M. C. Orilall, S. Hu¨ttner, H. Sai, U. Wiesner, U. Steiner, and H. J. Snaith, *Adv Funct Mater*, 2010, 20, 1787.

[11] Z. Lou, J. Deng, L. Wang, R. Wang, T. Fei and T. Zhang, *RSC Adv*., 2013, 3, 3131.

[12] J. Xing, H. Wei, E. Guo and F. Yang, *J. Phys. D: Appl. Phys.*, 2011, 44, 375104.

[13] X. Li , C. Gao , H. Duan , B. Lu , Y. Wang , L. Chen, Z. Zhang , X. Pan, and E. Xie, *small*, 2013, 9, 2005.

[14] M. Sun, X. Ma, X. Chen, Y. Sun, X. Cui and Y. Lin, *RSC Adv.*, 2014, 4, 1120.

[15] X. He, C. Huz, B. Feng, B. Wan and Y. Tian, *J. Electrochem. Soc.*, 2010, 157, 11, J381.

[16] T. Tsai, S. Chang, W. Weng, C. Hsu, S. Wang, C. Chiu, T. Hsueh and S. Chang, *J. Electrochem. Soc.*, 2012, 159, J132.

[17] J. Zou, Q. Zhang, K. Huang and N. Marzari, *J. Phys. Chem. C*, 2010, 114, 10725.

[18] B. Liu and E. S. Aydil, *J. Am. Chem. Soc.*, 2009, 131, 3985.

[19] S. Wang, W. Dong, R. Tao, Z. Deng, J. Shao, L. Hu, J. Zhu, X. Fang, *J. Power Sources*, 2013, 235, 193.

[20] H. Peng, J. Li, S. Li, and J. Xia, *J. Phys. Chem. C*, 2008, 112, 13964.

[21] E. Monroy, F. Omnes and F. Calle, *Semicond. Sci. Technol.*, 2003, 18, R33.

[22] K. Lv, M. Zhang, C. Liu, G. Liu, H. Li, S. Wen, Y. Chen, and S. Ruan, *J. Alloy. Compd.*, 2013, 580, 614.

[23] C. Soci, A. Zhang, X. Bao, H. Kim, Y. Lo, and D. Wang, *J. Nanosci. Nanotechno.*, 2010, 10, 1.

[24] R. O′Hayre, M. Nanu, J. Schoonman, and A. Goossens, *J. Phys. Chem. C*, 2007, 111, 4809.

[25] D. Cahen and G. Hodes, *J. Phys. Chem. B*, 2000, 104, 2053.

[26] H. Yu, S. Zhang, H. Zhao and H. Zhang, *Phys. Chem. Chem. Phys.*, 2010, 12, 6625.

[27] F. Guo and J. Huang, *Proc. of SPIE*, 2012, 8373, 83732k1.

[28] H. Seong, J. Yun, J. Jun, K. Cho and S. Kim, *Nanotechnology*, 2009, 20, 245201.